

## Effect of copper addition on the structure and properties of glass ceramics based on biogenic hydroxyapatite and sodium-borosilicate glass for bone tissue engineering

*O.Sych<sup>1</sup>, O.Kuda<sup>1</sup>, M.Demyda<sup>2</sup>, N.Pinchuk<sup>1</sup>, T.Tomila<sup>1</sup>,  
O.Bykov<sup>1</sup>, Y.Evysh<sup>1</sup>, A.Chodara<sup>3</sup>, W.Lojkowski<sup>3</sup>*

<sup>1</sup>I.Frantsevich Institute for Problems of Materials Science of NAS of Ukraine, Department of Functional Materials for Medical Application, 3 Krzhyzhanovsky Str., 03680 Kyiv, Ukraine

<sup>2</sup>National Technical University of Ukraine "I. Sikorsky Kyiv Polytechnic Institute", Department of Chemical Technology of Ceramics and Glass, 37 Peremogy Ave., 03056 Kyiv, Ukraine

<sup>3</sup>Institute of High Pressure Physics of the Polish Academy of Sciences, Laboratory of Nanostructures, 01-142 Warsaw, 29/37 Sokolowska Street, Poland

*Received December 3, 2019*

Bioceramics based on biogenic hydroxyapatite and sodium-borosilicate glass modified with 0; 0.5, 1.0, and 2.0 wt. % copper was prepared by two-stage sintering (1100 and 750°C). According to XRD results, it was established that the introduction of copper influences the volume of the unit crystalline cell of hydroxyapatite after both the first and second stages of sintering. After the latter, the formation of secondary phases ( $\text{NaCaPO}_4$ ,  $\text{Ca}_2\text{SiO}_4$ ,  $\text{Ca}_3(\text{SiO}_4)\text{O}$  and  $\text{Na}_2\text{Si}_3\text{O}_7$ ) was found for both copper-free and copper-modified composite materials. It was shown that the amount of copper does not affect the phase composition of samples after the final (second) sintering. It was established that copper addition decreases the total porosity of sintered samples (from 15.8 to 11.1 %) with forming an open porous structure as compared with copper-free bioceramics and makes it possible to increase the compressive strength by 1.7 times.

**Keywords:** hydroxyapatite, glasses, composites, bioceramics, copper.

**Вплив добавки міді на структуру та властивості склокераміки на основі біогенного гідроксиапатиту та натрійборосилікатного скла для інженерії кісткової тканини.**  
*О.Є.Сич, О.А.Куда, М.Б.Деміда, Н.Д.Пінчук, Т.В.Томила, О.І.Биков, Я.І.Євич, А.Ходара, В.Лойковський*

Біокераміку на основі біогенного гідроксиапатиту та натрійборосилікатного скла, модифікованого 0; 0,5, 1,0 та 2,0 мас. % міді, отримано методом двостадійного спікання (1100 та 750°C). За результатами РФА встановлено, що введення міді впливає на об'єм елементарної кристалічної комірки гідроксиапатиту як після першого, так і другого спікання. Після другого спікання утворення вторинних фаз ( $\text{NaCaPO}_4$ ,  $\text{Ca}_2\text{SiO}_4$ ,  $\text{Ca}_3(\text{SiO}_4)\text{O}$  і  $\text{Na}_2\text{Si}_3\text{O}_7$ ) зафіксовано як для "чистих", так і для модифікованих міддю композиційних матеріалів. Показано, що кількість міді не впливає на фазовий склад зразків після остаточного (другого) спікання. Встановлено, що додавання міді зменшує загальну пористість спечених зразків (з 15,8 до 11,1 %), утворюючи більш відкрито-пористу структуру у порівнянні з біокерамікою, що не містить міді, і дозволяє підвищити міцність на стиск у 1,7 разів.

Биокерамику на основе биогенного гидроксиапатита и натрийборосиликатного стекла, модифицированного 0; 0,5, 1,0 та 2,0 мас. % меди, получали методом двустадийного спекания (1100 та 750°C). По результатам РФА установлено, что введение меди влияет на объем элементарной кристаллической ячейки гидроксиапатита как после первого, так и второго спекания. После последнего образования вторичных фаз ( $\text{Na-CaPO}_4$ ,  $\text{Ca}_2\text{SiO}_4$ ,  $\text{Ca}_3(\text{SiO}_4)\text{O}$  и  $\text{Na}_2\text{Si}_3\text{O}_7$ ) зафиксировано как для "чистых", так и для модифицированных медью композиционных материалов. Показано, что количество меди не влияет на фазовый состав образцов после финального (второго) спекания. Установлено, что добавление меди уменьшает общую пористость спеченных образцов (с 15,8 до 11,1 %), образуя более открыто-пористую структуру по сравнению с биокерамикой, которая не содержит медь, и позволяет повысить прочность на сжатие в 1,7 р.

## 1. Introduction

Currently, various types of materials such as polymers, metals and their alloys, ceramics, bioglass, and various composites based on them are used for bone tissue engineering. As for bioceramics, hydroxyapatite (HA) is the most widely used as a synthetic and biogenic source due to its chemical affinity with bone and excellent biocompatible properties. Bioglass, in its turn, provides the best mechanical properties of bioceramics [1–6]. Such elements as silicon [7, 12], fluorine [13, 14], strontium [7, 15, 16], iron [17, 18], silver [19, 20], zinc [21, 22], copper [22, 24], etc. are introduced into the structure of HA ceramics to regulate bioactive properties, since it is known that the biochemical processes running in bone tissue are activated by trace elements, the content of which in the body is  $10^{-5}$ – $10^{-3}$  %.

As known, the human body contains a huge number of chemical elements. Most of them are found, to one degree or another, either in the bone tissue or in the blood. The trace elements are vital because in the absence or lack of them, the normal viability of the organism is disturbed [25]. The human body contains 0.072 g of copper. The minimum copper dose to be taken daily is 0.5–6.0 mg. Copper plays an important role in human life [26, 27]. A lack of copper leads to destruction of blood vessels and pathological growth of bones and defects in connective tissues. However, excessive copper leads to psyche violation and paralysis of some organs (Wilson's disease). A copper dose over 250 mg becomes toxic.

The authors [24] have shown that the introduction of copper in the form of 0.5–3.0 wt. % CuO into the porous borosilicate bioglass (mol. %)  $6\text{Na}_2\text{O}$ – $8\text{K}_2\text{O}$ – $8\text{MgO}$ – $22\text{CaO}$ – $36\text{K}_2\text{O}$ – $8\text{MgO}$ – $22\text{CaO}$ – $36\text{B}_2\text{O}_3$ – $18\text{SiO}_2$ – $\text{P}_2\text{O}_5$  does not lead to toxicity, and when implanted with a composite containing 3 wt. % CuO for a period of 8 weeks, significantly improves both angiogenesis and

bone regeneration compared to non-doped composites.

In [22], Cu-modified mesoporous bioglass was synthesized in the form of spheroidal nanoparticles. The introduction of up to 2 mol. % Cu into the bioglass structure resulted in a significant increase in the specific surface area; the material was additionally characterized by uniform mesopores, homogeneous distribution of copper, excellent biological properties, and the ability to stably release copper ions into the biological buffer solution. The antibacterial ability was rated as very effective for all strains of bacteria tested. The main role in the antibacterial action was prescribed to the copper ions released from the particles of the mesoporous copper bioglass, which exhibits a great potential as a multifunctional therapeutic agent for the prevention of infectious diseases and for stimulation of bone regeneration.

Thus, the introduction of copper into bioceramics and bioglass provides the material with antiseptic and bactericidal properties which positively affect subsequent implantation and stimulation of bone tissue regeneration.

The purpose of this work was to investigate regularities of the formation of the structure and properties of copper-modified bioceramics based on biogenic hydroxyapatite (BHA) and sodium-borosilicate glass.

## 2. Materials and Methods

The composition of the obtained and studied glass ceramics may be presented as a weight ratio of BHA and glass of 50/50. The sodium borosilicate glass phase had the following composition (wt. %): 26.1  $\text{Na}_2\text{O}$ ; 28.2  $\text{B}_2\text{O}_3$  and 45.7  $\text{SiO}_2$ .

To prepare glass ceramic samples, BHA obtained by calcination of cattle bones at 800°C was used, and sodium borosilicate glass was introduced in the form of the glass-forming components, namely silicon oxide  $\text{SiO}_2$ , sodium hydrocarbonate  $\text{NaHCO}_3$ , and boric acid  $\text{H}_3\text{BO}_3$  (all the

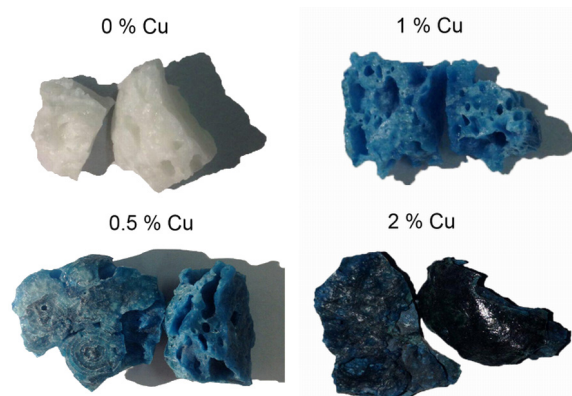


Fig. 1. Appearance of glass ceramics after the first sintering (1100°C).

starting materials were analytically pure, "Chemlaborractive", Ukraine). Four mixtures were prepared, three of which were added with 0.5; 1.0 and 2.0 wt. % of copper powder. The resulting mixtures were stirred and sintered in air at 1100°C for 1 h (first sintering). The sintered materials shown in Fig. 1, were crushed to a particle size of <160 µm, then cylindrical samples were formed by dry single-side air pressing at a pressure of 100 MPa, dried at 100°C for 2 h and sintered in air at 750°C for 1 h (second sintering). The used scheme for preparation of samples is presented in Fig. 2, and the appearance of bioceramic samples is shown in Fig. 3.

According to our previous investigations, the two-stage sintering process makes it possible to produce biocomposite samples with needed shape, high enough compression strength and solubility in vitro required for their practical use in reconstructive surgery. Moreover, the primary (first) sintering of a mixture of calcium phosphate and glass-forming components at 1100°C completely prevents foaming, volume growth in the system and the conversion of porosity from open to closed [28–31].



Fig. 2. Technological scheme of preparation of glass ceramic samples.

The phase composition of samples after first and second sintering was studied using X-ray diffraction analysis (XRD) with an Ultima IV (Rigaku, Japan) instrument equipped with a copper anode (wavelength 1.54 Å) and IR spectroscopy with a Fourier spectrometer FSM 1202 (InfraSpectr, Rus-

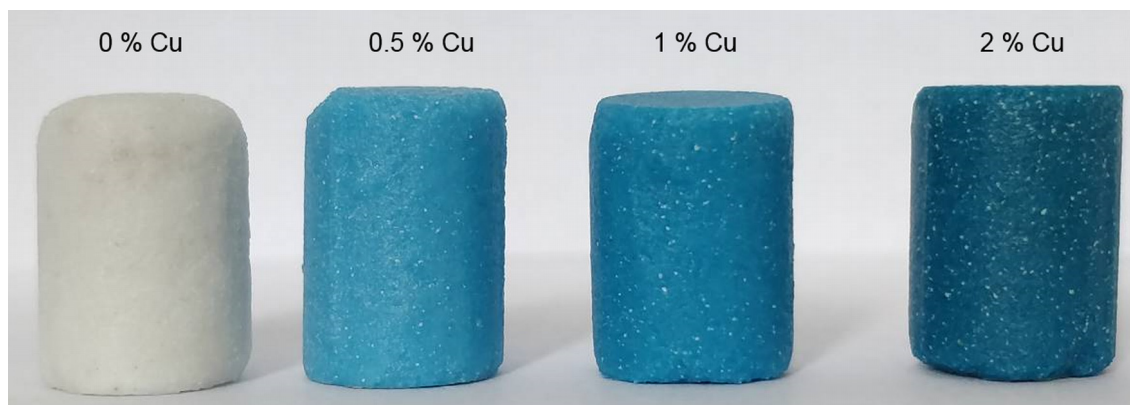


Fig. 3. Appearance of glass ceramic samples after the second sintering (750°C).

sia) in the frequency range of 4000–400  $\text{cm}^{-1}$  using a KBr tablet technology.

The chemical composition was analyzed by energy dispersive X-ray fluorescence elemental analysis (Expert 3L Analyzer, INAM, Ukraine).

The microstructure of the fracture of the samples was examined by scanning electron microscopy (SEM) with a microscope REM-106I (SEIMI, Ukraine).

The powder ability to be formed and densified under pressing and the effect of modifying additives on the pressing process was evaluated from the porosity values. The sintering process was investigated taking into account the volume shrinkage calculated from the sample geometric parameters (before and after sintering) and the data of mass loss during sintering.

Porosity was determined based on the data on the apparent and skeleton density. The first was calculated as a sample mass/volume ratio; the latter was determined using a helium pycnometer AccuPyc II 1340 (Micromeritics) at room temperature according to ISO 12154:2014.

The compressive strength was measured using a Ceram test system machine (Ukraine) at a loading speed of 1 mm/min.

### 3. Results and discussion

Fig. 4 shows the XRD results after first sintering of bioceramics at 1100°C. The diffraction pattern of the copper-free sample evidences that there is no noticeable interaction between the glass and BHA. The basic phase of the material is hexagonal HA  $\text{Ca}_5(\text{PO}_4)_3(\text{OH})$  (ICDD database, PDF file 09-0432), and the glass is X-ray-amorphous. The pattern also demonstrates very weak peaks of hexagonal  $\alpha'$ -tricalcium phosphate phases ( $\text{TCP}\alpha'$ - $\text{Ca}_3\text{PO}_4$ , PDF file 32-0176) and  $\gamma$ -calcium pyrophosphate (CPP)  $\gamma\text{-Ca}_2\text{P}_2\text{O}_7$  (ICDD database, PDF file 23-0871) formed during the high temperature sintering.

Addition of 0.5 % Cu as a modifying additive significantly changes the phase composition of the biomaterial during the first sintering (Fig. 4). Part of the BHA, obviously, becomes a basis for the formation of TCP in the form of whitlockite  $\text{Ca}_3(\text{PO}_4)_2$  (ICDD database, PDF file 03-0713), which becomes a basic crystalline phase of the biomaterial after first sintering. The main peaks of whitlockite coincide with those of the phase which is formed in a small amount as a result of the HA/copper interaction, that is,  $\text{Ca}_{19}\text{Cu}_{1.36}\text{H}_{2.24}(\text{PO}_4)_{14}$  (ICDD database, PDF file 89-4440); the

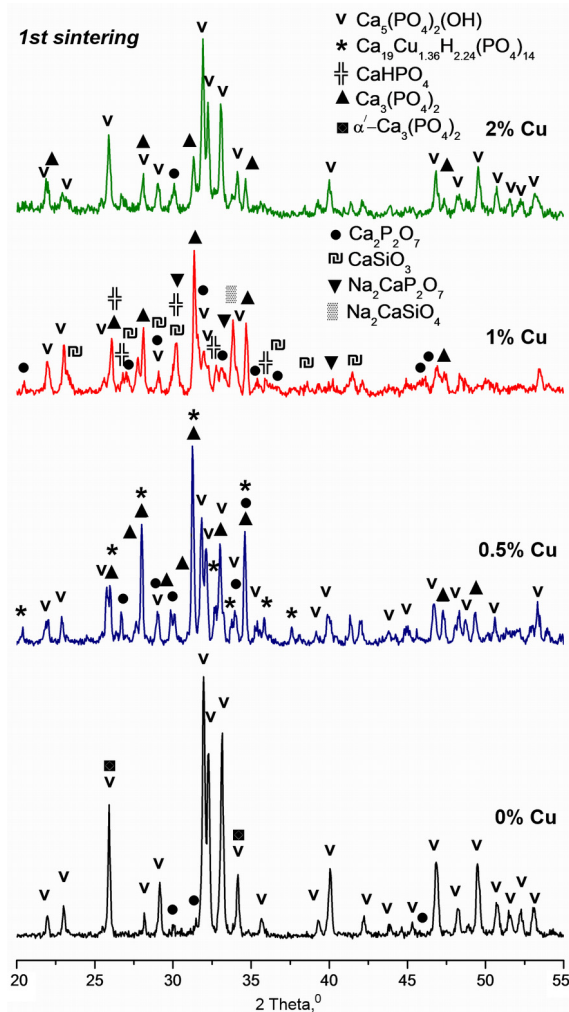


Fig. 4. XRD patterns of glass ceramics after the first sintering (1100°C).

presence of this phase is confirmed by the peak at  $2\theta \sim 37.5^\circ$  ( $2.389 \text{ \AA}$ ), which is not a "reflection" of other crystalline substances of this atomic system. Moreover, with the addition of 0.5 % Cu, the phases of HA ( $\text{Ca}_5(\text{PO}_4)_3(\text{OH})$ ), CPP ( $\gamma\text{-Ca}_2\text{P}_2\text{O}_7$ ), and TCP ( $\text{Ca}_3(\text{PO}_4)_2$  (ICDD database, PDF files 48-0488 and 09-0169) were identified.

An increase in the modifying additive content to 1 % leads to more significant changes in the biomaterial phase composition after the first sintering (Fig. 4). A characteristic feature of these changes is the further degradation of BHA, synthesis of a larger relative amount of TCP, and the appearance of monetite  $\text{CaHPO}_4$  (ICDD database, PDF file 71-1759). Another peculiarity of the phase composition is the formation of phases that are products of interaction of glass components with BHA, such as  $\text{Na}_2\text{CaSiO}_4$  (ICDD database, PDF file 35-

Table 1. Volume of crystal unit cell for HA in glass ceramics.

Stage of sintering	Volume of crystal unit cell (V), Å <sup>3</sup>			
	0% Cu	0.5% Cu	1.0% Cu	2.0% Cu
First	529.42	533.70	550.40	524.14
Second	529.44	529.64	530.46	526.21

0123), Na<sub>2</sub>CaP<sub>2</sub>O<sub>7</sub> (ICDD database, PDF file 48-0557), and wollastonite CaSiO<sub>3</sub> (ICDD database, PDF file 72-2284). It should be noted that the peak at 2 $\theta$  ~ 37.5 deg (2.389 Å), was not detected in the diffraction pattern; this fact may indicate the absence of Ca<sub>19</sub>Cu<sub>1.36</sub>H<sub>2.24</sub>(PO<sub>4</sub>)<sub>14</sub>. It can be assumed that this phase is intermediate during the conversion of BHA into copper-replaced TCP. Although replacement of calcium atoms with copper is not directly fixed by the XRD analysis, its presence is confirmed by the shift of the main peaks towards larger angles. The activity of BHA and its transformation into TCP may also result in forming an altered hexagonal lattice of HA. It can therefore be assumed that, in addition to the hexagonal HA (ICDD database, PDF file 09-0432), another hexagonal HA with smaller lattice parameters (ICDD database, PDF file 24-0033) is formed in the material as well.

After the introduction of 2 % copper into the biomaterial, HA again becomes, like in the copper-free material, the main phase (Fig. 4). The analysis of the ratio between the main phases (HA and TCP) in composite materials based on BHA and sodium borosilicate glass after the introduction of a modifying additive (copper) in the amount of 0, 0.5, 1.0 and 2.0 % revealed nonlinear changes in the phase composition after the first sintering. An increase in the copper content from 0 to 1.0 % leads to a gradual increase in the relative amount of TCP, but after addition of 2.0 % Cu, the main phase of the composite becomes HA, like in copper-free ceramics studied.

In addition to the above mentioned changes, a common feature of the crystalline structure of composite materials based on BHA and sodium borosilicate glass in the copper content range of 0–2.0 % after the first sintering (1100°C) is the change in the HA crystalline lattice parameters, which corresponds to the change in the unit cell volume (V) given in Table 1. The unit cell volume of HA in a copper-free composite is 529.42 Å<sup>3</sup>. The addition of 0.5 % Cu contrib-

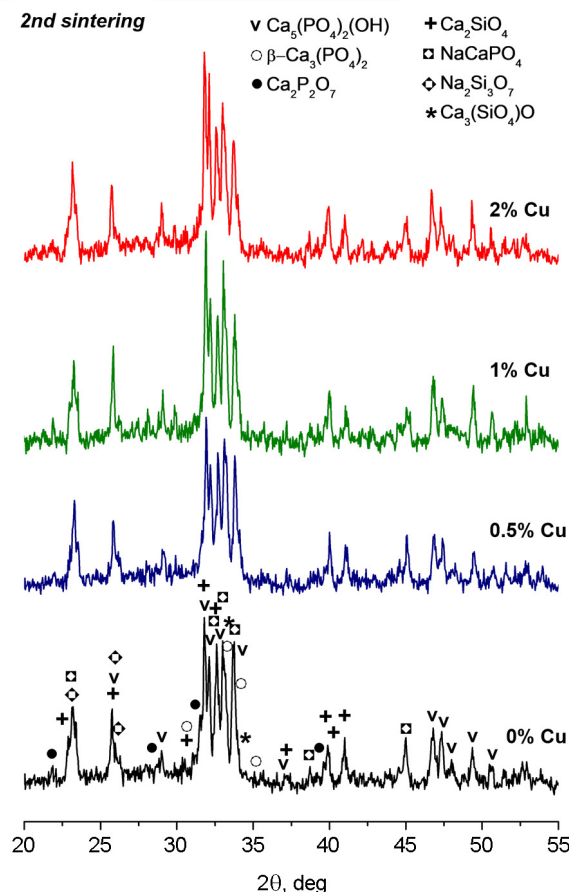


Fig. 5. XRD patterns of glass ceramics after the second sintering (750° C).

utes to formation of HA with  $V = 533.70$  Å<sup>3</sup>, and 1.0 % Cu causes the further growth of  $V$  to 550.40 Å<sup>3</sup>. A decrease in the unit cell volume is observed in the composite material containing 2.0 % Cu ( $V = 524.14$  Å<sup>3</sup>). It is known that during sintering, calcium atoms may be replaced with copper atoms. On the basis of the data given, one can conclude that this change becomes noticeable only at copper content of 2.0 %.

During the second sintering (750°C) of samples, further changes occur in their phase composition (Fig. 5). As demonstrated, after the second sintering of copper-free HA,  $V$  is 529.44 Å<sup>3</sup>. When 0.5 % Cu is added, HA is formed with  $V = 529.64$  Å<sup>3</sup>, that is, the volume slightly increases. Addition of 1.0 % Cu causes further growth of  $V$  to 530.46 Å<sup>3</sup>. However at 2.0 % Cu, a decrease in the unit cell volume ( $V = 526.21$  Å<sup>3</sup>) is observed, as after the first sintering. By comparing the materials with the same copper content after the first and the second stages of sintering, one can see

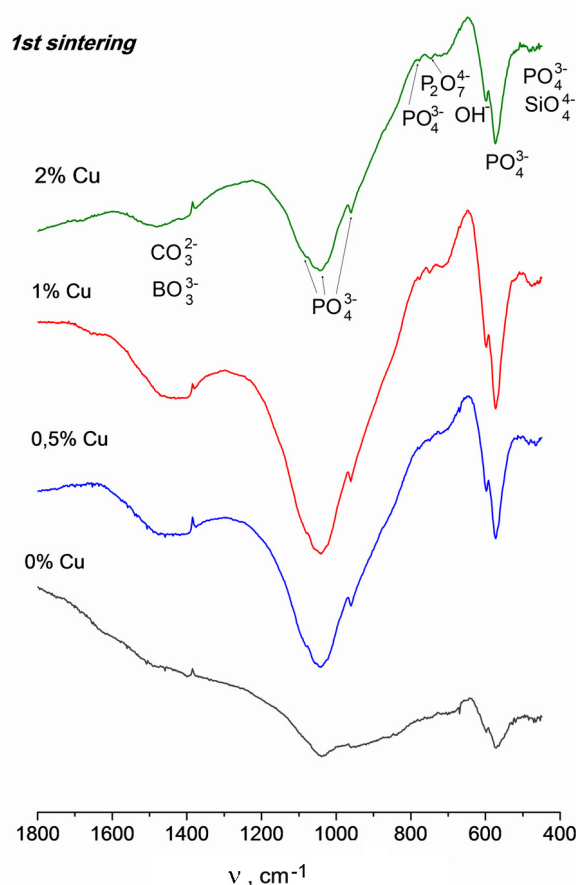


Fig. 6. IR spectra of glass ceramics after the first sintering (1100° C).

that at copper contents of 0.5 and 1.0 %, the HA unit cell volume decreases, whereas at 2.0 % Cu it somewhat increases. This fact indicates that the interaction of BHA with copper is noticeable only after the first (high temperature) sintering with the copper content of 2.0 %. During the second sintering, the interaction of BHA with sodium-borosilicate glass for both copper-free and copper-modified composite materials has a significant effect on the phase composition of the material, which leads to the formation of the following phases:  $\text{NaCaPO}_4$  (ICDD database, PDF file 76-1456);  $\text{Ca}_2\text{SiO}_4$  (ICDD database, PDF file 33-0302);  $\text{Ca}_3(\text{SiO}_4)\text{O}$  (ICDD database, PDF file 84-0594), and  $\text{Na}_2\text{Si}_3\text{O}_7$  (ICDD database, PDF file 38-0019) (Fig. 5). In the presence of copper, regardless of its amount, the phase composition of the samples after the second sintering changes insignificantly, as evidenced by the identical XRD patterns of the composite materials (Fig. 5).

The results of IR spectroscopy for bioceramics after first and second sintering are presented in Fig. 6 and 7, respectively.

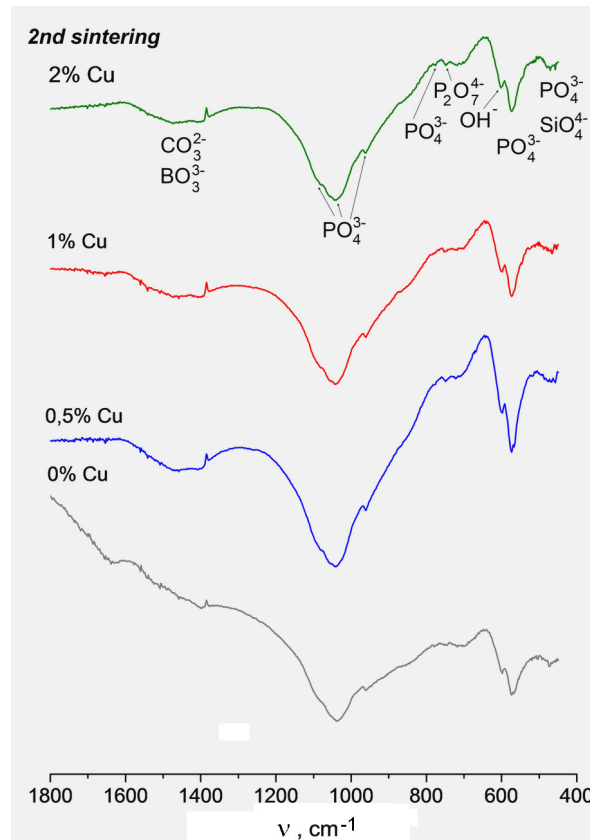


Fig. 7. IR spectra of glass ceramics after the second sintering (750° C).

They show broad and diffused absorption bands and the presence of fluctuations of the main  $\text{PO}_4^{3-}$  and  $\text{SiO}_4^{4-}$  groups in the copper-free composite sample based on BHA and sodium-borosilicate glass after the first sintering, which is consistent with our previous studies [11]. After the first sintering of a material with 0.5 % Cu, the IR spectra change. In particular, the intensity of all characteristic absorption bands increases and additional bands appear in the frequency range of 650–800  $\text{cm}^{-1}$  (Fig. 6). These changes indicate that there is an interaction in the system that changes the phase composition. The addition of 0.5 % Cu leads to Ca deficiency in the structure of BHA, and the calcium-deficient HA transforms into TCP, the amount of which increases in comparison with the copper-free composite. This change is manifested in an increase in the intensity of the absorption band at 962  $\text{cm}^{-1}$ . The  $\Delta\nu \sim 15 \text{ cm}^{-1}$  shift of the TCP specific absorption band at 1134  $\text{cm}^{-1}$  towards short waves with an increasing copper content indicates the formation of Cu-replaced TCP. The absorption band at 750  $\text{cm}^{-1}$  characterizes the P–O–P

Table 2. Properties of glass ceramic samples

Properties of glass ceramic samples		Amount of Cu, wt. %			
		0	0.5	1.0	2.0
Porosity of green bodies, $\pm 0.5$ %		31.8	31.4	31.2	30.8
Volume shrinkage, $\pm 0.05$ %		12.3	23.0	22.3	21.7
Mass loss, $\pm 0.01$ %		0.43	0.25	0.17	0.17
Skeleton density, $\pm 0.01$ g/cm <sup>3</sup>		2.41	2.56	2.55	2.56
Porosity, $\pm 0.5$ %	total	15.8	11.1	11.7	11.9
	open	6.2	6.5	5.7	7.9
Compression strength, $\pm 5$ MPa		120	178	213	184

vibrations for structural formations of  $P_2O_7$  and indicates the presence of CPP. The absorption bands at  $\sim 777$  and  $1050\text{ cm}^{-1}$  characterize the formation of wollastonite structures, while the weak band at  $\sim 487\text{ cm}^{-1}$  can be attributed to the characteristic Cu-replaced HA. These conclusions were confirmed by the XRD analysis.

After the second sintering, the shape of IR spectrum does not markedly change; this is due to the fact that the regions of the characteristic absorption bands overlap. Weak absorption bands at  $526\text{ cm}^{-1}$  and  $566\text{ cm}^{-1}$  may characterize the presence of calcium and sodium-silicates of different composition (Fig. 7).

After both sintering processes, weak broad bands are observed in the frequency range of  $1472\text{--}1400\text{ cm}^{-1}$ . They can be attributed to carbonate ion vibrations, and to valent B–O–B vibrations. XRD analysis did not reveal any carbonates or boron-containing structures. Thus, we can assume that their amount is negligible and refers to the remains of the initial components. Chemical analysis confirmed the amount of the modifying copper additive. Table 2 lists the results of determining the green body and bioceramic samples porosity depending on the copper content in the powder composition. As can be seen, the presence of copper does not significantly reduce the porosity. Herein the higher the copper content, the lower the porosity. After the second sintering, samples undergo a volume shrinkage and mass change. The introduction of copper into bioceramics increases the shrinkage of the samples, but reduces their mass loss. It also affects the sample skeleton density and porosity, reducing them. The copper content does not affect the density and total porosity. Despite the decrease in the total porosity, the introduction of copper increases the percentage of open porosity in

the samples, making the structure of porosity mostly open.

Fig. 8 demonstrates the structure of samples of copper-free and copper-modified bioceramics based on BHA; one can see that the glass-ceramic contains crystalline blocks (white areas), amorphous glass matrix (grey areas), and pores (black areas). The morphology is a porous structure with a pore size of  $2\text{--}100\text{ }\mu\text{m}$  for bioceramics both without copper and with 0.5, 1.0 and 2.0 % Cu. The surface and bulk of the composites contain numerous interconnected (open) and closed macro- and micro-pores. The sizes of the crystalline blocks present in the porous glass matrix are in the range of  $2\text{--}20\text{ }\mu\text{m}$  and do not depend on the presence and amount of the modifying additive. The only small difference between the copper-free and modified glass ceramics is the shape of crystalline phase blocks. In the copper-containing glass ceramics the block shape is generally round, while in the copper-free bioceramics, the blocks are both round and rectangular. This is confirmed by the XRD results, which showed certain changes in the phase composition of the crystalline component of glass ceramics after the introduction of copper. In general, the above micro-photos make it evident that the introduction of the modifying additive practically does not affect the structure of composite materials, which, in accordance with the results of XRD and IR spectroscopy, can be represented as a porous glass matrix with inclusions of HA and other phases.

Fig. 9 shows compression load diagrams for bioceramic samples depending on the copper content. All of the materials are characterized by the fragile type of destruction. The introduction of copper does not reduce the temporal resistance of samples during fracture, but at copper contents of 0.5 and 1.0 wt. %, the samples resist the destruction for a longer time as



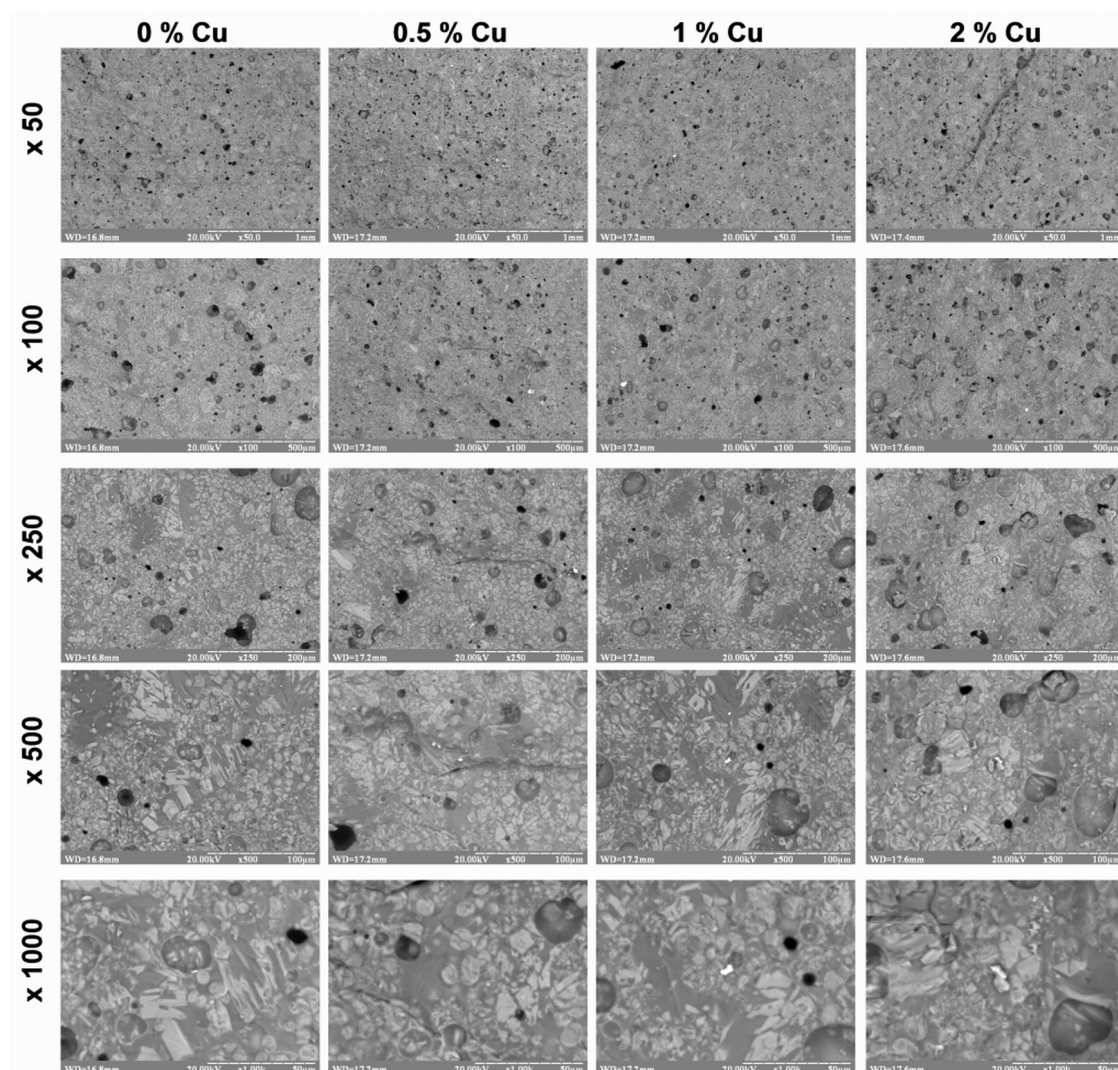


Fig. 8. SEM results for glass ceramics

compared with copper-free samples. The dependence of the compression strength on the copper content is presented in Table 3. The introduction of copper enhances the mechanical properties of samples from 120 to 213 MPa (1.7 times), herein an increase in the copper content affects the strength nonlinearly.

#### 4. Conclusions

Bioceramic samples based on biogenic hydroxyapatite and sodium-borosilicate glass (weight ratio of 50/50) were prepared by two-stage sintering (1100 and 750°C) and additionally modified with 0; 0.5, 1.0, and 2.0 wt. % copper.

The introduction of the modifying additive was established to result in decreasing the total porosity of sintered samples (from 15.8 to 11.1 %) with forming an open porous structure as compared with copper-free bioceramics.

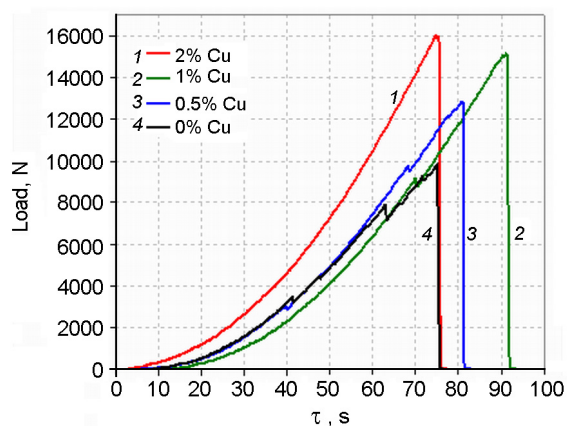


Fig. 9. Loading diagrams for glass ceramic samples

It was shown that introduction of copper influences the volume of a unit crystalline cell of hydroxyapatite (as the main crystalline phase of bioceramics) after both the



first and second sintering. After the latter, the formation of secondary phases such as  $\text{NaCaPO}_4$ ,  $\text{Ca}_2\text{SiO}_4$ ,  $\text{Ca}_3(\text{SiO}_4)\text{O}$  and  $\text{Na}_2\text{Si}_3\text{O}_7$  was observed for both copper-free and copper-modified composites. The amount of the modifying additive does not affect the phase composition of samples after the final (second) sintering.

It was established that introduction of the modifying additive into the composition of bioceramics practically does not affect the structure of composite materials (which can be represented as a porous glass matrix with inclusions of hydroxyapatite), but makes it possible to increase the compressive strength by 1.7 times.

The paper contains the results of studies conducted by Grant for monthly visits of Ukrainian scientists to Poland according to the Protocol to the Agreement on Scientific Cooperation between the National Academy of Sciences of Ukraine and Polish Academy of Sciences.

### References

1. G.Kaur, V.Kumar, F.Baino et al., *Mater. Sci. Eng. C*, **104**, 109895 (2019).
2. Y.Ma, H.Dai, X.Huang, Y.Long, *J. Mater. Sci.*, **54**, 10437 (2019).
3. P.-Y.Hsu, H.-C.Kuo, W.-H.Tuan et al., *Prog. Biomater.*, **8**, 115 (2019).
4. O.Sych, N.Pinchuk, *Process. Appl. Ceram.*, **1**, 1 (2007).
5. A.Iatsenko, O.Sych, T.Tomila, *Process. Appl. Ceram.*, **9**, 99 (2015).
6. O.R.Parkhomei, N.D.Pinchuk, O.E.Sych et al., *Powder Metall. Met. Ceram.*, **55**, 172 (2016).
7. C.Lin, H.Zhu, Y.Zeng, *Surf. Coat. Technol.*, **365**, 129 (2019).
8. X.Wang, S.Ihara, X.Li et al., *Colloid. Surf. B.*, **174**, 300(2019).
9. O.Sych, A.Iatsenko, T.Tomila et al., *AdvNano-BioM&D*, **2**, 223 (2018).
10. E.E.Sych, *Glass Ceram.*, **72**, 107 (2015).
11. E.E.Sych, N.D.Pinchuk, V.P.Klimenko et al., *Powder Metall. Met. Ceram.*, **54**, 67 (2015).
12. O.Sych, N.Pinchuk, V.Klymenko et al., *Process. Appl. Ceram.*, **9**, 125 (2015).
13. P.Nasker, A.Samanta, S.Rudra et al., *J. Mech. Behav. Biomed. Mater.*, **95**, 136 (2019).
14. O.Sych, A.Iatsenko, H.Tovstonoh et al., *Functional Materials*, **24**, 46 (2017).
15. T.-H.Huang, C.-T.Kao, Y.-F.Shen et al., *J. Mater. Sci.:Mater. Med.*, **30**, 68 (2019).
16. O.Kuda, N.Pinchuk, O.Bykov et al., *Nanoscale Res. Lett.*, **13**, 155 (2018).
17. O.Kaygili, *J. Aust. Ceram. Soc.*, **55**, 381 (2019).
18. O.M.Otychenko, T.Ye.Babutina, D.P.Ziatkevich et al., *Functional Materials*, **25**, 695 (2018).
19. A.C.Marsh, N.P.Mellott, N.Pajares-Chamorro et al., *Bioact. Mater.*, **4**, 215 (2019).
20. C.R.Mariappan, N.Ranga, *Ceram. Int.*, **43**, 2196 (2017).
21. D.Zamani, F.Moztarzadeh, D.Bizari, *Int. J. Biol. Macromol.*, **137**, 1256 (2019).
22. C.F.Marquesa, S.Olheroa, J.C.C.Abrantes, *Ceram. Int.*, **43**, 15719 (2017).
23. K.Magyari, Zs.Pap, Z.R.Toth, *J. Sol-Gel Sci. Technol.*, **91**, 634 (2019).
24. M.J.Robles-Aguilaa, J.A.Reyes-Avendano, M.E.Mendoza, *Ceram. Int.*, **43**, 12705 (2017).
25. S.E.Etok, E.Valsami-Jones, T.J.Wess et al., *J. Mater. Sci.*, **42**, 9807 (2007).
26. Z.Radovanovic, B.Jokic, D.Veljovic et al., *Appl. Surf. Sci.*, **307**, 513 (2014).
27. R.K.Singh, S.Kannan, *Mater. Sci. Eng. C*, **45**, 530 (2014).
28. N.D.Pinchuk, L.A.Ivanchenko, *Powder Metall. Met. Ceram.*, **42**, 357 (2003).
29. E.E.Sych, N.D.Pinchuk, L.A.Ivanchenko et al., *Nanosistemy, Nanomaterialy, Nanotehnologii*, **7**, 263 (2009).
30. O.Sych, N.Pinchuk, L.Ivanchenko, *Process. Appl. Ceram.*, **3**, 157 (2009).
31. E.E.Sych, N.D.Pinchuk, L.A.Ivanchenko, *Powder Metall. Met. Ceram.*, **49**, 153 (2010).